Numerical Study on Dynamic Response of Tension-moored Floating Structure Using IB-VOF Method

Peng Wei[1], Lee Kwang-Ho[2] and Norimi Mizutani[3]

[1]Department of Civil Engineering, Nagoya University, pengwei@civil.nagoya-u.ac.jp
[2]Department of Civil Engineering, Nagoya University, leekh@civil.nagoya-u.ac.jp
[3]Department of Civil Engineering, Nagoya University, mizutani@civil.nagoya-u.ac.jp

In this work, a numerical model using an immersed boundary (IB) method and volume of fluid (VOF) method is proposed to estimate the interactions between free-surface waves and submerged floating body, which is inclinedly moored. The IB method is applied to handle solid object boundaries which are replaced with a proper force in the Navier-Stokes equations imposed on the body surface. The VOF method is employed to track the free surface. The finite displacements of the breakwater such as sway, heave and roll in very small time step are considered using the Newton's laws of motion. The validity of the developed model in the evaluation of free surface and the motions of floating breakwater is supported by the comparisons of numerical results and available experimental data.

Key words: *Wave-structure interaction; IB method; VOF method; Submerged floating breakwater*

1. INTRODUCTION

Floating breakwaters can give a good alternative solution to protect harbors from wave attack compared to traditional gravity-type breakwaters with several advantages, e.g. eco-friendliness, lower construction cost, convenience of transportation and installation. The understanding of dynamics of a floating breakwater, including the response of the structure such as sway, heave and roll, under wave action is very important in designing the structure not only for the efficiency of dissipating wave energy but also for the safety of the breakwater structure.

The earlier work on the dynamics of floating structures depends largely on the potential theory in the frequency domain. However, there are two shortages in the application of these kinds of models. One is the difficulty in simulating large-scale motions of floating body. The other one is the assumption of irrotational flow, which generates difficulty in reproducing the rotational motion of floating body and vortex formed around the structure. Mizutani et al. (2004) proposed a VOF-based numerical model using Fractional Area Volume Obstacle Representation (FAVOR) method to simulate the dynamics of the moored floating breakwater. However, in the FAVOR method, the mass conservation cannot be fully satisfied when treating the movable solid boundary such as the floating body. Another issue is the high computational cost due to the reconstruction of the complex geometry of the solid structure. Lee and Mizutani (2007, 2009) presented a numerical wave flume model based on Immersed Boundary (IB) method, which is capable of handling interface problems with complex geometry on a standard regular Cartesian grid. Lee et al. (2008) reported that IB method can successfully simulate the dynamic behavior of the vertically moored tension leg floating body.

In this paper, we extend the numerical model proposed by Lee et al. (2007, 2009) to the inclinedly moored floating body. Three freedoms of

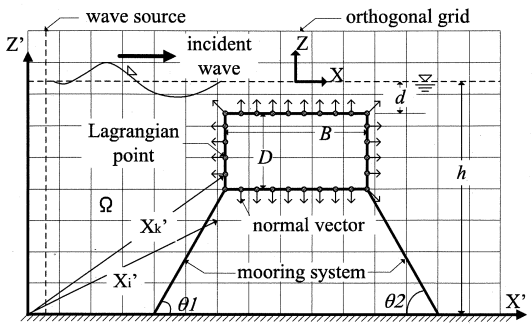

Fig. 1 Schematic illustration of computation domain.

floating body motion are considered as sway, heave and roll. Moreover, experimental results are utilized to validate the numerical model.

2. NUMERICAL MODLE

(1) Governing equations

In the 2D wave-structure interaction, the flow of an incompressible viscous fluid in a Cartesian domain Ω, as illustrated in Fig. 1, is governed by the continuity equation and modified Navior-Stokes equations, given by

$$\frac{\partial u_i}{\partial x_i} = Q \tag{1}$$

$$\frac{Du_i}{Dt} = -\frac{1}{\rho}\frac{\partial p}{\partial x_i} + 2\nu\frac{\partial D_{ij}}{\partial x_j} - \frac{2\nu}{3}\frac{\partial Q}{\partial x_i} - g_i - \gamma u_i \delta_{i2} + L_i \tag{2}$$

where x_i donates the x or the z orthogonal Cartesian coordinate, u_i is the velocity component (u, w) in the i direction, p is pressure, ρ is the fluid density, t is time, g is the acceleration due to gravity, v is the kinematic viscosity coefficient of the water, γ is a wave dissipation factor, which is equal to zero except for the sponge zones, D_{ij} is the velocity stress tensor, and Q is the source term at the source position $x=x_s$, $Q=q(z,t)/\Delta x_s$ where q is the flux density and Δx_s is the grid width at the source position. Furthermore, in Eq. (2), L_i is the Eulerian force (Lima E Silva et al., 2003) in the i direction, which corresponds to the effect of a solid body on the flow, determined by

$$L_i = \int_\Omega \tilde{L}_{ki}\delta(x_i - x_k)dx_k \tag{3}$$

where $\tilde{L}_{ki}$ is the force density at the Lagrangian points x_k, and $\delta(x_i - x_k)$ is a Dirac delta function.

Also, the advection equation of VOF function F is used to capture the free water surface, as follows:

$$\frac{\partial F}{\partial t} + \frac{\partial (u_i F)}{\partial x_i} = FQ \tag{4}$$

(2) IB method

The IB method was originally introduced by Peskin (1972) to simulate blood flows in mitral valves, and was later developed to solve problems in various fields including incompressible fluid flows (e.g., Fadlun et al., 2000; Kim et al., 2001; Lee and Mizutani, 2007, 2009). The main advantage of the IB method is the simplified gird generation without coordinate transformation, overlapping and mapping of meshes.

In the present model, the boundary of obstacle is replaced with a set of discrete control points x_k (Lagrangian points). The force density $\tilde{L}_{ki}$ is computed over these points, and then distributed to the nearby Cartesian grid points by a certain distribution function.

a) Evaluation of forcing term

It is noted that the forcing term L_i is added to the momentum equation to represent the embedded solid boundary. The imposed force components must be determined before the solving of momentum equation. In this study, the PVM method (Lima E Silva et al., 2003) is preferred due to its simplicity and lower calculation cost. In the PVM method, the added forcing term is calculated explicitly, and is broken into different terms, while each term has a specific physical meaning. The Lagrangian force field $\tilde{L}_{ki}$, in Eq. (3) is expressed by

$$\tilde{L}_{ki} = \frac{u_{ki} - u_{f\,ki}}{\Delta t} + u_{kj}\frac{\partial u_{ki}}{\partial x_j} - \nu\frac{\partial^2 u_{ki}}{\partial x_j^2} + \frac{1}{\rho}\frac{\partial p_k}{\partial x_i} \tag{5}$$

where u_{ki} and p_k are the interface velocity components and pressure over the interface, respectively, the subscript i represents the direction in the Cartesian coordinate system and x_k is the location of the Lagrangian point. The forcing term is taken apart as acceleration forcing, inertial forcing, viscous forcing and pressure forcing as shown in the RHS of Eq. (5).

In the calculation of Eq. (5), the fluid velocity must be equal to the interface velocity, which guarantees the no-slip condition. The spatial derivatives of the velocity and pressure in the Lagrangian force term will be obtained by a polynomial at each Lagrangian point k using the fluid particle velocity and pressure around the Lagrangian point (Lima E Silva et al., 2003; Lee and Mizutani, 2007, 2009).

b) Distribution of forcing term

From the Eq. (5), the Lagrangian force term can be calculated and a smooth distribution function is needed to link them to the Eulerian grids. The well-discretized Dirac delta function (Griffith and Peskin, 2005) is used as (Eq. (6) ~ Eq. (9)). Then, a two-step projection method (Chorin, 1968) is adopted to solve the governing equations.

$$L_i = \sum_k \tilde{L}_{ki} D_i \Delta l_p^2 \tag{6}$$

$$D_i(x_k) = \prod_i \left[\frac{f_i[(x_k - x_i)/\Delta x_i]}{\Delta x_i} \right] \tag{7}$$

where the function f is defined as:

$$f(r) = \begin{cases} \tilde{f}(r) & ; \ |r| \le 1 \\ 0.5 - \tilde{f}(2-r) & ; \ 1 < |r| \le 2 \\ 0 & ; \ |r| > 2 \end{cases} \tag{8}$$

$$\tilde{f}(r) = \frac{3 - 2|r| + \sqrt{1 + 4|r| - 4|r|^2}}{8} \tag{9}$$

(3) Dynamics of the floating body

It is considered that the weight of the floating body is much smaller than the buoyancy forces acting on it vertically, which means the slack state of the mooring chains will not occur. The dynamic properties of the submerged floating breakwater due to its interaction with wave are formulated (Fig. 2). The wave forces acting on the surfaces of the breakwater H_1~H_4 and V_1~V_4 can be calculated by

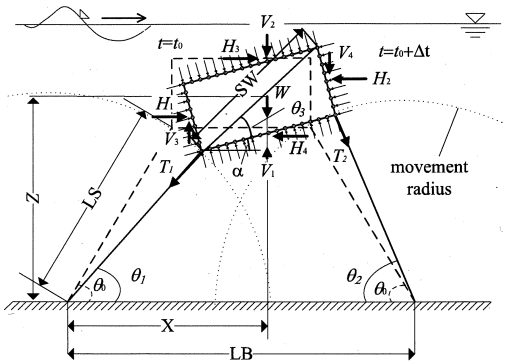

Fig. 2 Calculation of the floating body dynamics.

integrating the pressures on the corresponding surface. For the floating body, considering the moments acting on the centre of gravity, resultant horizontal and vertical force acting on the body, the following equations can be derived:

$$\sum M_{c.g} = \sum M_{cg.x} + \sum M_{cg.z} + \sum M_{cg.T} = J_{FB}\alpha_{FB} \tag{10}$$

$$\sum F_X = m\alpha_x = H_1 + H_3 - H_2 - H_4 + 2(T_2\cos\theta_2 - T_1\cos\theta_1) \tag{11}$$

$$\sum F_Z = m\alpha_Z = V_1 + V_3 - W - V_2 - V_4 - 2(T_2\sin\theta_2 + T_1\sin\theta_1) \tag{12}$$

where $\sum M_{cg.x}$, $\sum M_{cg.z}$, $\sum M_{cg.T}$ represent the summation of moment governed by the horizontal

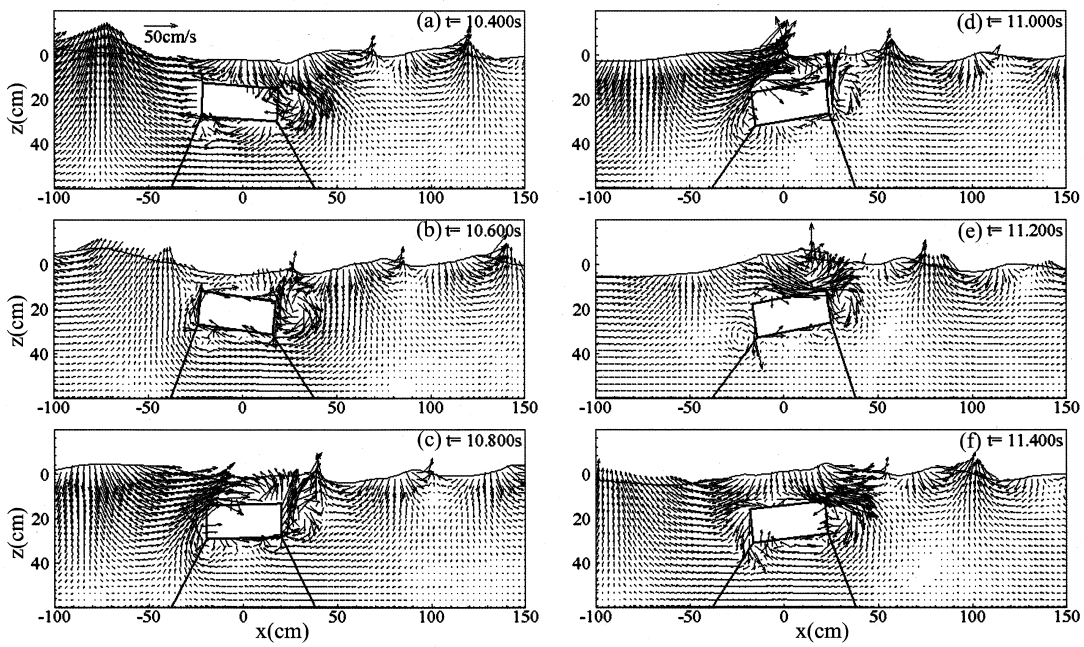

Fig. 3 Numerical model results of water particle velocity (cm/s) field around the inclinedly moored floating breakwater (case 2).

wave forces, vertical wave forces and the mooring forces respectively, J_{FB} is the mass moment of inertia of the floating body, α_{FB}, α_x, α_z are the accelerations of angle α, horizontal direction and vertical direction respectively; m is the mass of the floating body.

Considering no slack condition, two additional equations can be derived from the geometry in Fig. 2 as:

$$LS^2 = (X - \frac{SW}{2}\cos(\theta_3 + \alpha))^2 + (Z - \frac{SW}{2}\sin(\theta_3 + \alpha))^2 \quad (13)$$

$$LS^2 = (LB - X - \frac{SW}{2}\cos(\theta_3 - \alpha))^2 + (Z - \frac{SW}{2}\sin(\theta_3 - \alpha))^2 \quad (14)$$

By solving above five equations (Eq. (10) ~ Eq. (14)) simultaneously, the unknown parameters α_{FB}, α_x, α_z, T_1 and T_2 can be calculated. Finally, the sway, heave and roll displacements are estimated using α_{FB}, α_x and α_z values.

3. RESULTS AND DISCUSSION

Laboratory experiments were carried out in a two-dimensional wave tank at Nagoya University. In the experiments, a rectangular shaped pontoon type submerged floating breakwater (length: 0.4 m; width: 0.68 m; height: 0.15 m; weight: 28.6 kg) with the mooring chain (length: 0.36 m) was used. Experimental data is employed to estimate the performance of the developed model for two cases, case1: wave period T_i=0.9 seconds; wave height H_i=0.038 m; depth of wave tank h=0.60 m; distance from the static water level to the top surface of floating breakwater d=0.137 m; inclined angle θ_0=60°; wave steepness H_i/L=0.03; case2: T_i=1.2 s, H_i=0.085 m, h=0.60 m, d=0.137 m, θ_0=60°, H_i/L=0.04. In the computation, a uniform grid system with Δx=Δz=0.01 m and the time interval of 0.001 s was employed.

Figure 3 shows the transient velocity field and the corresponding free surface position during one wave period at the interval of 0.2 s. Utilizing the water surface profile, complex forms such as the wave breaking phenomenon can be monitored using the proposed model (Fig. 3(e)). Further, a vortex is observed near the floating body when the incident wave is propagating over the submerged floating breakwater. Also, the corresponding positions of the breakwater are captured in this figure, which show an oscillation due to the interaction with waves.

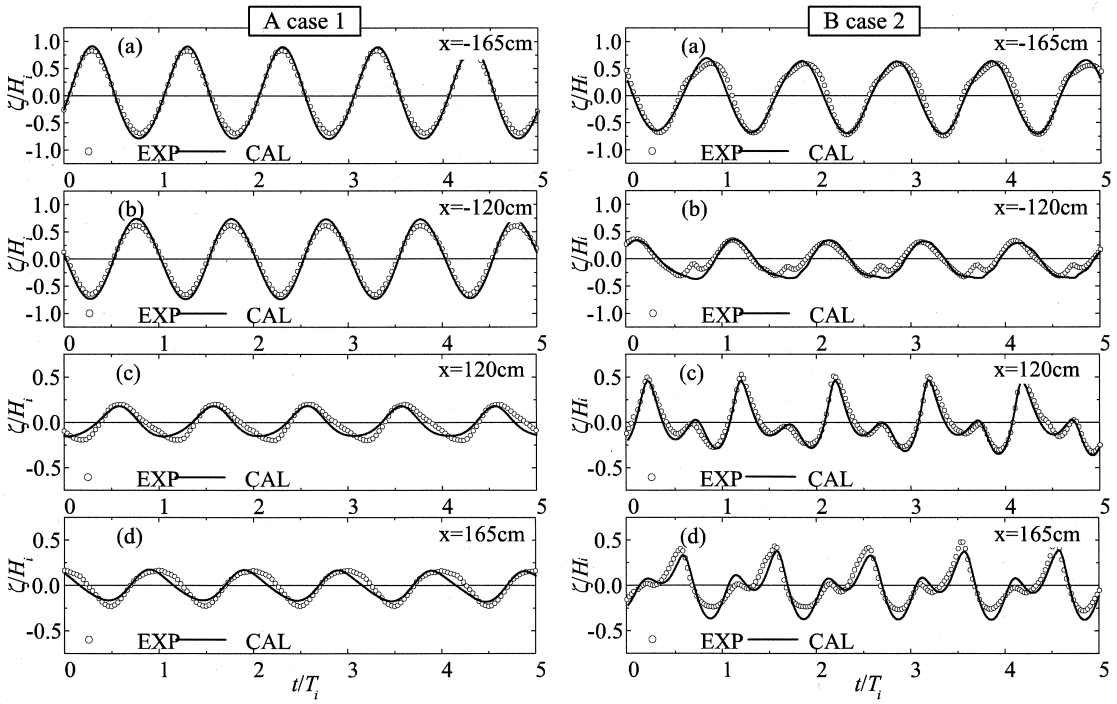

Fig. 4 Comparison between numerical and experimental results of the dimensionless water surface profiles.

The time series water surfaces at four points of offshore and onshore sides for case 1 and case 2 are predicted and shown in Fig. 4(A) and (B) respectively. The experiment measures are added for comparison for five wave cycles and a good agreement is achieved, which demands the good performance of VOF method in evaluating the free surface. In Fig. 4(A), the water surface profiles of onshore side are nearly symmetric, which means the affection of nonlinear interaction is indistinctive due to smaller wave height in case 1. On the other hand, in Fig. 4(B), the water surfaces at onshore side show inconsistent variation in both estimated and measured values. This variation indicates a complex form in the reformed area after the wave breaking and a secondary crest is created due to the wave-floating body interaction.

Figure 5 shows the comparisons between the simulated displacements of the floating body and the experiment results as function of the dimensionless time. A good agreement is observed between them. Even for the heave motion, the results are reasonable considering the inevitable measurement errors during experiments. Therefore, the presented model is validated to be a reliable dynamic simulator in mimicking the interaction of solid object with wave.

4. CONCLUSION

A two-dimensional numerical model was developed to analyze the interaction between wave and pontoon type rectangular shaped submerged floating breakwater which is anchored with the chain system. The model incorporated IB method for treating the floating breakwater and the VOF method for tracking the free surface. Also, the displacements (sway, heave and roll) of the floating body under wave action were estimated using this model. The validity of the developed model is well supported by the comparisons of estimated values and experimental measurements in evaluating water surface profiles and motions of the submerged floating breakwater.

ACKNOWLEDGMENT: This work was financially supported by the Grant-in-Aid for Scientific Research from the Japan Society for the Promotion of Science (B-20760326).

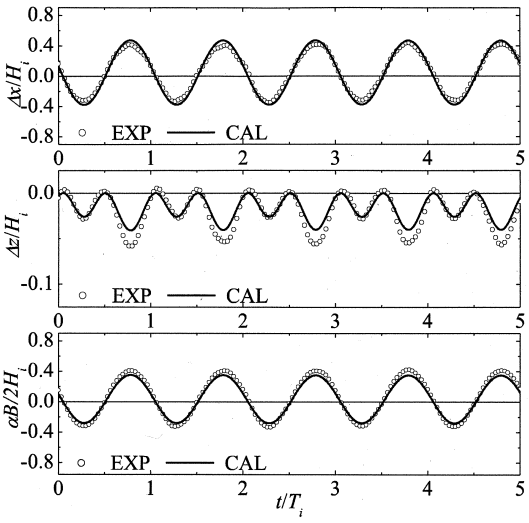

Fig. 5 Comparisons between numerical and experimental results of displacements of the floating body (case 1).

REFERENCES

Chorin, A. J. (1968): Numerical solution of the Navier-Stokes equations, *Math. Comp.*, Vol. 22, pp. 745-762.

Fadlun, E.A., R. Verzicco, P. Orlandi and J. Mohd-Yusof (2000): Combined immersed-boundary finite-difference methods for three-dimensional complex flow simulations, *Journal of Computational Physics*, Vol. 161, No. 1, pp. 35-60.

Griffith, B.E. and C. S. Peskin (2005): On the order of accuracy of the immersed boundary method: Higher order convergence rates for sufficiently smooth problems, *Journal of Computational Physics*, Vol. 208, pp. 75-105.

Kim, J., D. Kim and H. Choi (2001): An immersed-boundary finite-volume method for simulations of flow in complex geometries, *Journal of Computational Physics*, Vol. 171, No. 1, pp. 132-150.

Lee, K.-H. and N. Mizutani (2007): Numerical wave flume with immersed boundary method and its applicability in wave fields simulation around a horizontal circular cylinder, *Annual Journal of Coastal Engineering*, JSCE, Vol. 54, pp. 821-825. (in Japanese)

Lee, K.-H., N. Mizutani and M. Goto (2008): Numerical simulation of dynamic behavior of tension leg floating body using IB method, *Annual Journal of Coastal Engineering*, JSCE, Vol.55, pp.891-895. (in Japanese)

Lee, K.-H. and N. Mizutani (2009): A numerical tank using direct-forcing immersed boundary method and its application to wave force on a horizontal cylinder, *Costal Engineering Journal*, Vol. 51, No. 1, pp. 27-48.

Lima e Silva, A. L. F., A. Silveria-Neto and J. J. R. Damasceno (2003): Numerical simulation of two dimensional flows over a circular cylinder using the immersed boundary method, *Journal of Computational Physics*, Vol. 351, pp. 351-370.

Mizutani, N., M.A. Rahman, D.S. Hur and H. Shimabukuro (2004): VOF simulation for dynamic behavior of submerged floating breakwater and wave deformation considering finite displacement, *Annual Journal of the Costal Engineering*, JSCE, Vol. 51, pp. 701-705. (in Japanese)

Peskin, C. S. (1977): Numerical analysis of blood flow in the heart, *Journal of Computational Physics*, Vol. 25, pp. 220-252.

(Received June 16, 2010)